Chemical Engineering Journal 203 (2012) 440–446

Contents lists available at SciVerse ScienceDirect

Chemical Engineering Journal

journal homepage: www.elsevier.com/locate/cej

Preparation of tetraoxalyl ethylenediamine melamine resin grafted-carbon fibers for nano-nickel recovery from spent electroless nickel plating baths

Guan-Ping Jin [a,b,*], Xiu-Li Wang [a], Ya Fu [a], Yan Do [a,b]

[a] Department of Application Chemistry, School of Chemical Engineering, Hefei University of Technology, Hefei 230009, PR China
[b] Anhui Key Laboratory of Controllable Chemistry Reaction & Material Chemical Engineering, Hefei 230009, PR China

HIGHLIGHTS

- Tetraoxalyl ethylenediamine melamine resin could uptake nickel ions from spent electroless nickel plating baths.
- Tetraoxalyl ethylenediamine melamine resin grafted-carbon fibers.
- Electrochemical preparation of nano-nickel at the treated carbon fibers.
- Recovery of nano-nickel.

GRAPHICAL ABSTRACT

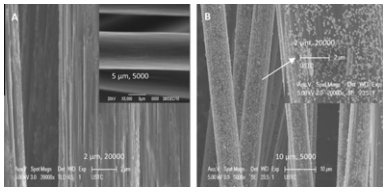

ARTICLE INFO

Article history:
Received 17 April 2012
Received in revised form 6 July 2012
Accepted 9 July 2012
Available online 20 July 2012

Keywords:
Chelate resin grafted-carbon fibers
Recovery of nickel
Spent electroless nickel plating baths
Electrodeposition

ABSTRACT

A novel nickel recovery method was designed using tetraoxalyl ethylenediamine melamine chelate resin grafted-carbon fibers (MFT/CFs) from the spent electroless nickel plating baths. The process involved inoculation of tetraoxalyl ethylenediamine melamine chelate resin at CFs, the adsorption and eletrodeposition of Ni^{2+} at MFT/CFs. Ethylenediamine was covalently modified at CFs by constant potential, tetraoxalyl ethylenediamine was grafted at the CFs by amidation reaction, then melamine, formaldehyde and tetraoxalyl ethylenediamine could be polymerized at the CFs. The MFT/CFs showed an excellent uptake effect for Ni^{2+} with a pseudo-second order model. The interaction mechanism between Ni^{2+} and active sites has been interpreted as chelation. Nano-nickel coated-MFT/CFs materials could be obtained by electrodeposition (Ni/MFT/CFs). The present materials were carefully examined by fourier transform infrared spectroscopy, field emission scanning electron microscope, X-ray diffraction, X-ray photoelectron spectroscopy and electrochemistry techniques. The characterization results suggested the formation of Ni/MFT/CFs with a good electrocatalysis for ethanol oxidation.

© 2012 Elsevier B.V. All rights reserved.

1. Introduction

Electroless nickel plating is an indispensable surface finishing technology, widely used in electronic and automobile industries [1,2]. A large amount of the spent electroless nickel plating baths containing high concentrations of phosphite, hypophosphite, organic acids, especial nickel, is becoming a serious environmental problem. The recovery of nickel from the spent electroless nickel plating baths has attracted much attention in terms of environmental protection and economic value. Up to now some treatment methods have been reported for the nickel recovery. For example: alkaline precipitation [3], ion exchange [4,5], solvent extraction [6,7], electrodialysis [8], electrolytes [9–11] and activated carbon adsorption [12]. Although these methods have obtained much useful effect, there are some difficulties including heavy metal sludge, regeneration chemicals as well as membrane fouling. On the basis of these facts, it is significant to develop new effective nickel recycling technique to best use the spent electroless nickel plating baths.

Since carbon fibers (CFs) have outstanding mechanical properties, chemical stability, adsorption, conduction and surface area. Nowadays it has been widely applied on mechanical and aviatic

* Corresponding author at: Department of Application Chemistry, School of Chemical Engineering, Hefei University of Technology, Hefei 230009, PR China. Tel./fax: +86 551 2901450.
E-mail address: jgp@hfut.edu.cn (G.-P. Jin).

1385-8947/$ - see front matter © 2012 Elsevier B.V. All rights reserved.
http://dx.doi.org/10.1016/j.cej.2012.07.055

equipment [13], interesting studies for us lay in heavy metal wastewater treatment, metal catalyst support and electrochemistry [14–17]. For examples: Chergui and coworker revealed that cyclam-functionalized polyglycidyl methacrylate could be grafted on CFs by atom transfer radical polymerization using aryl diazonium salt initiators. The resulting material showed an excellent uptake towards Cu^{2+} [14]. Kara and Arai prepared nickel-coated CFs using sodiumhypophosphite as reducing agent [15,16]. Xu reported that CFs could be readily treated by electrochemical method [17]. Moreover, El-Ghaffar and co-works reported that tetraoxalyl ethylenediamine modified melamine resin show good adsorption effect to Cu^{2+} [18].

In this context, we aimed at designing novel chelate resin grafted-CFs to directly prepare nano-nickel coated-CFs materials using the spent electroless nickel plating baths.

2. Experimental

2.1. Apparatus and chemicals

All electrochemical experiments were performed with a CHI 660 B electrochemical workstation (Chenhua, Shanghai, China). A conventional three-electrode electrochemical system was used for all electrochemical experiments, which consisted of a working electrode (CFs), a twisted platinum wire counter electrode, a silver wires or saturated calomel reference electrode (SCE). Field emission scanning electron microscope (FE-SEM) images were obtained on a JSM-600 field emission scanning electron microanalyser (JEOL, Japan). X-ray diffraction (XRD) data of the samples were collected using a Rigaku D/MAX-rB diffractometer with Cu Kα radiation. XPS spectra were recorded by using an ESCALABMK2 spectrometer (Vg Corporation, UK) with Mg-Alpha X-ray radiation as the source for excitation. Infrared spectra were measured at IR 200 (America, Nicolet). The average pore sizes and the specific surface area of MFT/CFs were measured using Nova 2200e Surface Area & Pore Size Analyzer (Quantachrome Instrument, America). pH meter model was measured at HI 255 (Shanghai Leici instruments).

Polyacrylonitrile-carbon fibers (CFs) were obtained from Dingfeng Carbon Fibers Fabrication Company of Yixing (China, Wuxi), one truss CFs have about 3000 branches with a diameter of 7 ± 1 μm, it was been snipped at 10 mm long in following experiments. Melamine, formaldehyde (37%), oxalic acid, xylene, ethylenediamine and all other chemicals were Chemical Reagent Company of Shanghai products (China, Shanghai). A stock solution of 5 mM EDTA was prepared and standardized against a solution of $MgSO_4{\cdot}7H_2O$ using Eriochrome Black-T (EBT) as an indicator. HNO_3 and NaOH were used to change the acidity of the medium. The composition of electroless nickel spent plating baths was shown in Table 1, the content for Ni(II) is 0.107 M, and the pH is 4.8. S 930 chelating resin with iminodiacetic acid, which is bound in a macroporous polystyrene matrix (Purolite International Co., LTD).

2.2. Graft of tetraoxalyl ethylenediamine modified melamine resin at CFs

Tetraoxalyl ethylenediamine (TOED) was prepared according to the previously reported method [19]. Oxalic acid and ethylenediamine with molar ratio (4:1) were mixed in 250 mL round-bottom flask filtrated with Dean & Stark apparatus. The mixture was heated under reflux with xylene until the theoretical amount of water has been collected. The reaction mixture was then cooled to room temperature, filtrated and dried at 50 °C under vacuum. The solid collected was recrystallized from a suitable solvent.

200 trusses CFs immerged in 50 mL of mixed acid solution of nitric acid and perchlorate acid (7:3). The mixed solution was ultrasonically agitated for 7 h to form carboxyl-carbon fibers [20]. The CFs were washed with doubly distilled water to a neutral pH, washed with acetone, and dried in air; then in 250 mL beaker, 20 trusses CFs were treated in a solution containing 1 mM ethylenediamine/0.1 M lithium perchlorate/acetonitrile at a constant potential of 1.5 V in 1 h, which were reduced at −1.1 V in 0.1 M KCl/enthanol/H_2O (enthanol:H_2O, v:v = 1:1) in 1 h to form ethylenediamine modified CFs.

In 250 mL round flask, tetraoxalyl ethylenediamine was inoculated at tetraoxalyl ethylenediamine modified CFs by amidation reaction in 1 mM tetraoxalyl ethylenediamine at 75 °C for 2 h; after that, melamine was added to the flask, it was heated in water bath with stirring at 75 °C for 2 h; then formaldehyde and sodium dodecylsulfate were added to the flask, tetraoxalyl ethylenediamine, melamine and formaldehyde at molar ratio of 1:1:1.5, and sodium dodecylsulfate at mass ratio of 0.5%; there after the temperature was raised to 90 °C for 2 h with continuous stirring. The tetraoxalyl ethylenediamine modified melamine resin coated-carbon fibers were collected, washed thoroughly with hot water, cold water, ethanol and acetone, and dried in air (labeled MFT/CFs).

2.3. Preparation of Ni/MFT/CFs from the spent electroless nickel plating baths

In 250 mL beaker 100 mL spent electroless nickel plating baths was adjusted by 0.1 M NaOH at pH 5.2, 1 mL 1 mM $PdCl_2$ was added to the beaker to form dissociative Ni^{2+} with stirring at 40 °C for 1 h; after that, 20 trusses MFT/CFs were immerged in the beaker to adsorb Ni^{2+} with stirring at 55 °C for 30 min; Ni^{2+}-MFT/CFs was used as working electrode at a potential of −0.7 V for 30 s in 0.1 M KCl to obtain nano-nickel coated-carbon fibers (labeled as Ni/MFT/CFs).

3. Result and discussion

3.1. Characterization of MFT/CFs

FT-IR spectra. IR spectra of relative materials including acid treated CFs (a), melamine (b), TOED (c) and MFT/CFs (d) were investigated in Fig. 1. The carbonyl (C═O) stretch at 1630 cm^{-1}

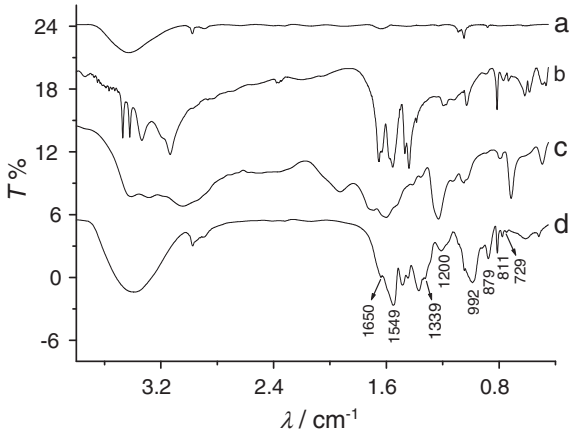

Fig. 1. IR spectra of relative materials including acid treated CFs (a), melamine (b), TOED (c) and MFT/CFs (d).

Table 1
Composition (M) and pH value of the model spent bath pH 4.8.

$NiSO_4$	Na_2SO_4	NaH_2PO_2	NaH_2PO_2	Lactic acid	H_2SO_4	Na_2HPO_3
0.107	0.35	0.24	0.24	0.30	0.20	0.70

could be seen at acid treated CFs (a). For melamine (b), the double peaks at 3468 and 3418 cm^{-1} can be assigned to the symmetrical and asymmetrical stretching vibrations of NH_2 group. The peaks at 1650–1437 cm^{-1} are caused by framework vibration in the molecules. The peak at 810 cm^{-1} is attributed to the out-of-plane ring deformation [21]. For TOED (c), the peak at 3317 cm^{-1} and 1553 cm^{-1} are due to the N—H stretch attached to themethylene bridge and N—H bend bridging in the secondary amine [18]. It could be readily seen that the spectra of MFT/CFs (d) show common peaks due to the existence of similar groups. For example, the peak at 1650 cm^{-1} matches to carbonyl (C=O) stretch; 1630–1437 cm^{-1} and 810 cm^{-1} relate to melmine; 3317 cm^{-1}, 1553 cm^{-1}, 1339 cm^{-1} and 717 cm^{-1} can be traced back to TOED. The structure of MFT/CFs could be suggested in Fig. 2 (1). Ethylenediamine was covalently modified at CFs firstly. Tetraoxalyl ethylenediamine was inoculated at the CFs secondly. Then tetraoxalyl ethylenediamine melamine chelate resins could be polymerized at the CFs (MFT/CFs).

The physical and textural properties of MFT/CFs were further investigated, and the results were summarized in Table 2. The surface area of MFT/CFs (1167 $m^2\ g^{-1}$) is larger than that of CFs. Moreover, water regain factor was investigated; *W*% represents the percentage of water held intrinsically by MFT/CFs. For water regain determination, MFT/CFs samples were dried at 50–60 °C until complete dryness then weighed again. To calculate this factor, the following equation was applied in Eq. (1). Where W_w and W_d are weights (g) of the wet and dried resin respectively. Water regain values are about 0% for CFs, (1.1 ± 0.1)% for acid treated CFs, (3.7 ± 0.5)% for MFT/CFs, suggesting an improved hydrophilic character.

$$W\% = 100(W_w - W_d)/W_w \quad (1)$$

3.2. Preparation of Ni/MFT/CFs

3.2.1. Optimum preparation conditions

Optimum preparation conditions for Ni/MFT/CFs including pH, temperature and adsorption time were investigated using cyclic voltammetry (CV), respectively. On the different conditions, one truss MFT/CFs immerged in 10 mL the spent electroless nickel plating baths to adsorb Ni^{2+}, after cleaning by ethanol and water, nanonickel was electrodeposited at MFT/CFs in 0.1 M KCl (Ni/MFT/CFs). The Ni/MFT/CFs shows a pair of redox peaks marching to NiOOH ↔ $Ni(OH)_2$ (0.75/0.21 V) in 0.1 M NaOH in Fig. 3B. Since the current response balance needs about continuous 50 cycles, the optimum conditions could be obtained by the oxidation peak currents at the 50th cycle.

The initial 4.8 pH value of the spent electroless nickel plating baths were adjusted from 2 to 6 by addition of HNO_3 and NaOH. At 300 rpm and 25 ± 1 °C for 1 h, Fig. 3A shows that the oxidation peak response at 0.75 V is very small at pH < 2.5, it is obviously increased with a increasing pH until reaching a maximum value at pH 5.2 (1.48 mA), thus pH 5.2 is optimum. These phenomena could be proved in following experiment.

The uptake of Ni^{2+} at different temperature (*T*) was done from 25 °C to 75 °C at 300 rpm pH 5.2 for 1 h. As shown in Fig. 3A, inset a, there is not any response at *T* < 30 °C the oxidation peak current at 0.75 V is gradually increased with a increasing temperature until reaching a maximum value at 55 °C (1.43 mA), then it displays a flat up to 65 °C, and an obvious decrease after *T* > 65 °C (0.92 mA). Thus the optimum temperature is 55 °C.

The uptake of Ni^{2+} at different adsorption time intervals was done at pH 5.2, 300 rpm and at 55 °C. The inset b in Fig. 3A shows that the oxidation peak currents are increased with the delay of

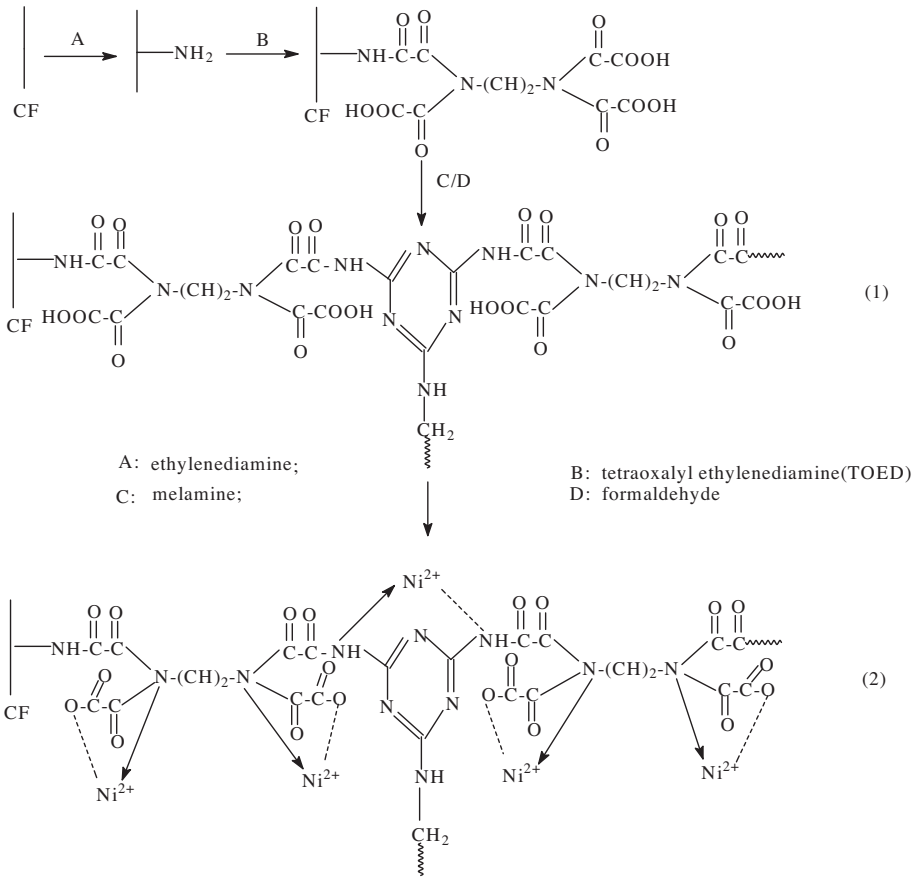

Fig. 2. Proposed scheme of tetraoxalyl ethylenediamine melamine chelating resin grafte-CFs (1) and chelate mechanism of MFT/CFs with Ni^{2+} (2).

Table 2
Physical and textural properties of MFT/CFs.

Sample	Surface area ($m^2\ g^{-1}$)	Pore volume ($cm^3\ g^{-1}$)	Pore diameter (nm)	Water content (%)
MFT/CFs	1167	0.37	50 ± 20	3.7 ± 0.5
CFs	1020	0.29	3 ± 1	1.1 ± 0.1

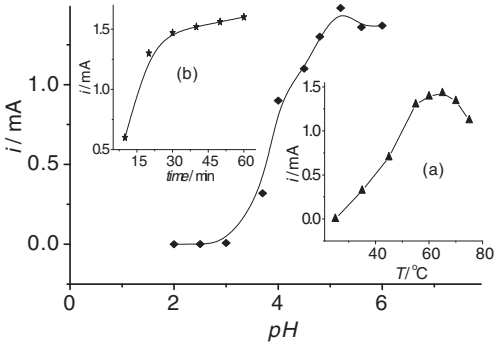

Fig. 3a. Oxidation peak currents of Ni adsorbed at MFT/CFs depend on pH, adsorption temperature (a) and adsorption time (b). Initial $[Ni^{2+}] = 0.107$ M in the spent electroless plating bath.

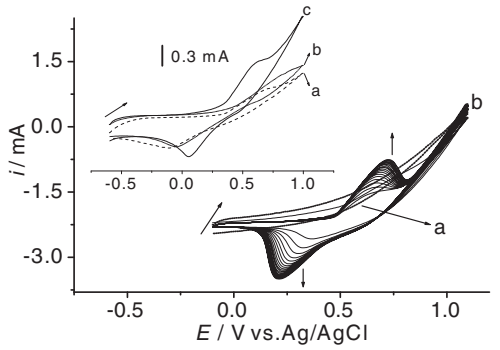

Fig. 3b. CVs of Ni/MFT/CFs in continuing 50 scan, CVs (50^{th}) of CFs (a), MFT/CFs (b) and Ni/MFT/CFs (c) in 0.04 M C_2H_5OH/0.1 M NaOH; Scan rate: 50 mV s^{-1}.

adsorption time from 10 to 30 min; it keeps a slow increase after 30 min (1.52 mA). Thus the optimum adsorption time is 30 min. It is noticeable that the optimum adsorption time could be prolonged with the decrease of the concentration of Ni^{2+} in the spent baths, when the concentration was 0.02 M and 0.002 M, the time would be delayed to 45 min and 120 min.

3.2.2. Removal of Ni^{2+} in spent electroless nickel plating baths

The amount of Ni^{2+} adsorbed per unit mass of the adsorbent was evaluated using the mass balance Eq. (2): where q_t (mg g^{-1}) is the amount adsorbed per gram of adsorbent per gram at time t (min), C_0 is the initial concentration of Ni^{2+} in the spent electroless nickel plating baths, C_t is the concentration of Ni^{2+} at time t of adsorption (mg L^{-1}), W is the mass of the adsorbent used (g), and V (L) is the initial volume of the spent electroless nickel plating baths. On the optimum conditions (55 °C, 30 min, pH 5.2), the adsorption content was estimated by balance ($n = 5$). An average quality was at a range of 45 ± 2 mg Ni/1 g MFT/CFs.

$$q_t = (C_0 - C_t)V/W \quad (2)$$

Moreover, the adsorption content of Ni^{2+} at acid treated CFs and commercial S930 chelating resin were investigated to compare uptake effect in the spent electroless nickel plating baths, the values were 16 ± 2 and 27 ± 2 mg Ni/1 g in same conditions, respectively. It illustrated that present MFT/CFs was better for the Ni recovery. Actually, the uptake value at S930 was lager than that in literature (about 12 mg Ni/1 g) [22], the reason was probably relative to the part deposition of Ni^{2+} at the surface of chelating resin in the spent electroless nickel plating baths.

3.2.3. Characterization of Ni/MFT/CFs

As shown in Fig. 3B, there are not any peaks at bare MFT/CFs (a) in 0.1 M NaOH. However, a pair of redox peaks (b, 0.72/0.21 V) could be seen at Ni/MFT/CFs matching to the transformation of Ni to NiOOH and $Ni(OH)_2$ [20]. The redox peaks currents are gradually increasing in continuous scan in continuous cycle, and reach balance at about 50 cycles, suggesting transformation finish. The electrocatalysis of Ni/MFT/CFs towards redox of ethanol was investigated in inset. In comparison with that of CFs (a) and MFT/CFs (b), the Ni/MFT/CFs (c) shows much better electrocatalysis with an obvious increased current response.

After MFT/CFs immerged in the spent electroless nickel plating baths to adsorb Ni^{2+}, nano-nickel was electrodeposited at MFT/CFs in situ. XRD spectra of Ni/MFT/CFs confirm the presence of nickel nanoparticles in Fig. 4. The peak at 44.4° could be assigned to Ni^{2+}, and the most common nanoparticles on the CFs are face-centered cubic (FCC). The average crystallite size is 3.98 nm using Scherrer's equation from the width at half peak maximum. It is noticed that the peak is wider, it probably contributes to the formation of NiP nanoparticles and in line with the literature [15].

FE-SEM was utilized to investigate the surface morphology of Ni/MFT/CFs in Fig. 5. As shown in Fig. 5A (MFT/CFs) and inset (CFs), the surface of MFT/CFs is rough compared with that of original CFs with a diameter of 7 ± 1 μm. However, plentiful nano-islands could been readily seen at Ni/MFT/CFs with a size of 80 ± 60 nm in Fig. 5B and inset, signifying the formation of nano-nickel at MFT/CFs.

Fig. 6 shows the XPS spectra of acid treated CFs (a), MFT/CFs (b), Ni/MFT/CFs (c). There are two peaks for C_{1s} (285.8 eV) and O_{1s} (531.7 eV) in curve *a*. A topical N_{1s} peak appears at 399.3 eV in curve b, suggesting the existence of nitrogen function at MFT/CFs. As shown in curve c, A topical Ni_{2p} peak could be seen at 884 eV compared with that in curve *a* and *b*, implying the deposition of nickel on MFT/CFs. Meanwhile, P_{2p} peak at 133.1 eV can also be observed, which probably come from the spend electrolesss

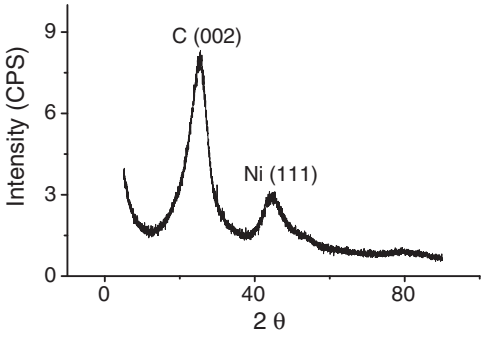

Fig. 4. XRD spectra of Ni/MFT/CFs.

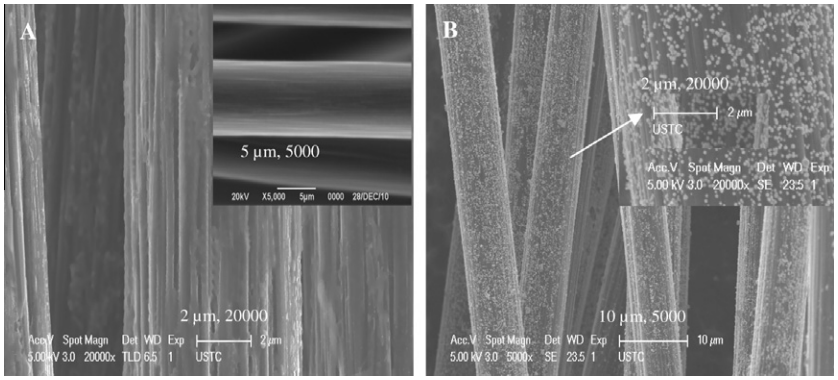

Fig. 5. FE-SEM of MFT/CFs (A), CFs (A, inset) and Ni/MFT/CFs (B).

nickel plating bath, and suggesting the existence of NiP in Ni/MFT/CFs.

3.3. Uptake studies for equilibrium pH, kinetic studies, adsorption isotherms, selectivity and regeneration

The uptake studies of MFT/CFs towards Ni^{2+} such as equilibrium pH, kinetic studies, adsorption isotherms, selectivity and regeneration were investigated in the spent electroless plnting baths, respectively, where the residual concentration of Ni^{2+} was determined by the titration against 5 mM EDTA using EBT as an indicator [18].

Metal ions adsorption from aqueous solution into a resin is a pH dependent process due to pH influence on both the chemistry of metal ions and resin functional groups. Since TOED molecule in the MFT resins has EDTA-like (Ethylenediaminetetra-actic acid) structure, it was expected that TOED moiety could form stable complexes with Ni^{2+} [23]. This behavior is clear in Fig. 7. The adsorption of Ni^{2+} was increased dramatically with increasing pH until reaching a maximum value (0.77 mM/g) at equilibrium pH 5.2. It is notable that the pH decreased to 5.0 after 40 min. This may be attributed to two points; on the one hand, the chelation of Ni^{2+} by the TOED group immobilized on the CFs results in the release of two hydrogen ions for each Ni^{2+} ion in addition to water of hydration, on the other hand, it is the partial deprotonation of coordinating groups (carboxylate and amine). In neutral or slightly acidic media, the uptake probably attributes to the formation of resin-metal ion complex, which causes increase of the acidity of the medium due to release of H^+ from coordinating carboxylate groups [18]. The scheme could be suggested in Fig. 2 (2).

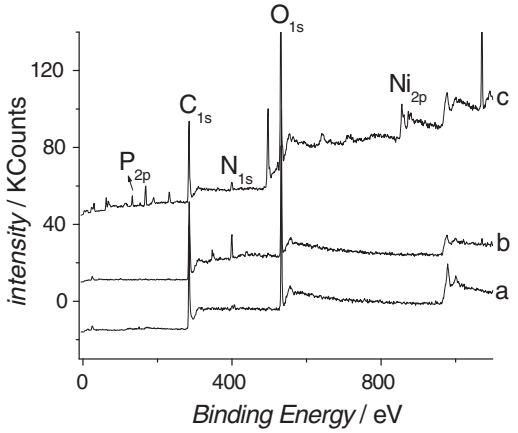

Fig. 6. XPS of acid treated CFs (a), MFT/CFs (b) and Ni/MFT/CFs (c).

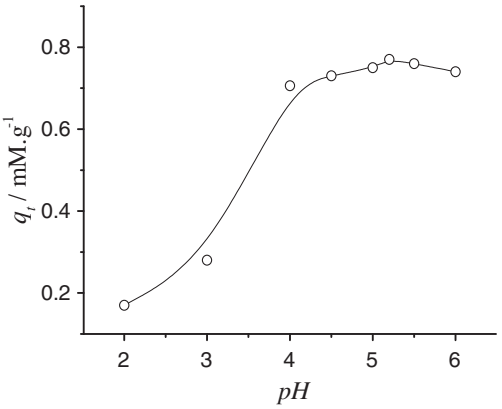

Fig. 7. The uptake of Ni^{2+} depend on pH at MFT/CFs at 55 °C and 30 min. Initial $[Ni^{2+}]$ = 0.107 M in the spent electroless plating bath.

The kinetics of Ni^{2+} removal on 10 trusses MFT/CFs was investigated at initial concentrations of $[Ni^{2+}]$ = 0.107 M at pH 5.2 and 55 °C. The adsorption-time data were treated according to pseudo-second-order [24] and intraparticle diffusion [25]. The pseudo-second-order rate constants (k_2) and the amount of Ni^{2+} adsorbed at equilibrium (q_e) were calculated from the slope and intercept of the plots of t/q_t versus t according to Eq. (3) [24]. Where k_2 (g mM min^{-1}) is the pseudo-second-order rate constant, q_e is the amount of Ni^{2+} adsorbed (mM g^{-1}) at equilibrium, and q_t is the amount of the adsorption (mM g^{-1}) at anytime t. The kinetics of the removal process could be seen in Fig. 8 and inset (a). The dates were summarized in Table 3. The theoretical q_e values are the equilibrium concentrations of Ni^{2+} in the adsorbed MFT/CFs, assuming 100% of Ni^{2+} was removed. The calculated q_e values are close to the theoretical ones, showing quite good linearity with R^2 above 0.997. For comparison, the adsorption-time data in Table 3 were treated according to pseudo-first order too [26]. The calculated q_e and R^2 values were 0.591 and 0.949. Therefore, the adsorption kinetics follows the pseudo-second-order model [24], suggesting a chemisorption process [27].

$$t/q_t = 1/k_2 q_e^2 + (1/q_e)t \quad (3)$$

Due to the porous nature of the present MFT/CFs, pore diffusion (intraparticle diffusion) in addition to surface diffusion (film diffusion) may contribute to the overall adsorption, they are slower, would be the rate-determining step. The kinetic behavior of MFT/CFs on the rate of sorption reaction was confirmed from the plot between the quantity of metal ion adsorbed at different time

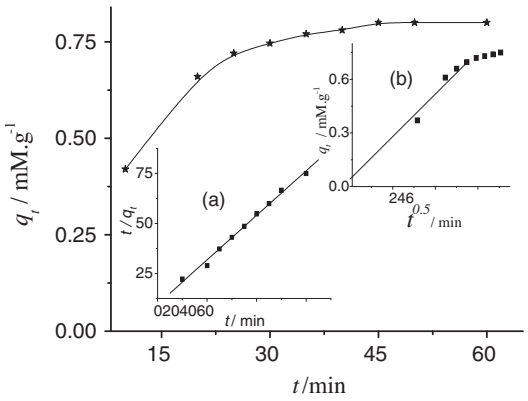

Fig. 8. The uptake of Ni^{2+} depend on time at MFT/CFs at pH 5.2 and 55 °C. Inset A: Pseudo second-order kinetics of the uptake of Ni^{2+}at MFT/CFs. Inset B: the intraparticle diffusion kinetics model for the adsorption of Ni^{2+}at MFT/CFs. Initial [Ni^{2+}] = 0.107 M in the spent electroless plating bath.

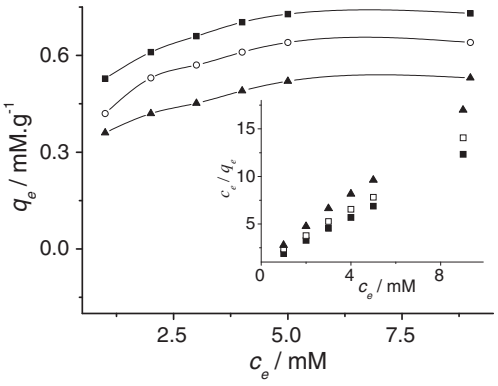

Fig. 9. Adsorption isotherms for the adsorption of Ni^{2+} at MFT/CFs at 35 °C (▲), 45 °C (○) and 55 °C (■) at pH 5.2. Inset: plotting C_e/q_e against C_e.

intervals (q_t) and square root of time ($t^{0.5}$) in Eq. (4), which originated from Fick's second law [18]: where X represents the boundary layer diffusion effects (external film resistance); K_{dif} is the intraparticle diffusion rate constant (mM g^{-1} min^{-1}), which is usually used to compare mass transfer rates. As shown in Fig. 8, inset (b), the straight line indicates that the rate of adsorption is controlled by intraparticle diffusion process [25]. As the value of X decreases the effect of external diffusion on the reaction rate decreases. The calculated (X) is a positive value, this value for (X) in the 2nd case indicates the dependence of the reaction rate to a small extent on external film diffusion. This may be attributed to the lower hydrophilicity of MFT/CFs. This external film diffusion in 2nd case shifts the reaction rate of the adsorption of Ni^{2+} on MFT/CFs towards pseudo-second order one.

$$q_t = X + K_{dif} t^{0.5} \tag{4}$$

Adsorption isotherms of Ni^{2+} removal on 10 trusses MFT/CFs were investigated at 35, 45 and 55 °C in Fig. 9. The adsorption curves show maximum uptake values for Ni^{2+} at 0.53, 0.64 and 0.73 mM/g, respectively. The adsorption data were plotted according to Langmuir Eq. (5) [18]. Where C_e is the concentration of metal ions in solution (mM), qe is the metal ions concentration in the resin phase at MFT/CFs (mM/g), Q_{max} the maximum adsorption capacity (mM/g) and K_L is the Langmuir binding constant which is related to the energy of adsorption (L/mM). All concentrations refer to equilibrium conditions. Plotting C_e/q_e against C_e gives a straight line with a slope and an intercept equals $1/Q_{max}$ and $1/K_L Q_{max}$, respectively. The values of K_L and Q_{max} at different temperatures are summarized in Table 4. The value of Q_{max} (obtained from Langmuir plots) at 55 °C is mainly consistent with that experimentally obtained, indicating that the adsorption process is mainly monolayer.

$$C_e/q_e = C_e/Q_{max} + 1/K_L Q_{max} \tag{5}$$

The degree of suitability of MFT/CFs towards Ni^{2+} was estimated from the values of separation factor constant (R_L), which gives indication for the possibility of the adsorption process to proceed. $R_L > 1.0$ unsuitable; $R_L = 1$ linear; $0 < R_L < 1$ suitable; $R_L = 0$ irreversible [28]. The value of R_L can be calculated from the relation (6). Where K_L (L/mmol) is the Langmuir equilibrium constant and C_0 (mM) is the initial concentration of metal ion. The values of R_L lies between 0.045 and 0.40 indicating the suitability of the studied resins as adsorbents for Ni^{2+} from the spent electroless nickel plating bath.

$$R_L = 1/1 + K_L C_0 \tag{6}$$

The observed increase in both values of Q_{max} and K_L at elevated temperature indicates the endothermic nature of the adsorption process. The values of K_L at different temperatures were treated according to van't Hoff Eq. (7) [29]. Where $\Delta H°$ (J/mol) and $\Delta S°$ (J/mol K) are enthalpy and entropy changes, respectively, R is the universal gas constant (8.314 J/mol K) and T is the absolute temperature (in Kelvin). Plotting ln K_L against $1/T$ gives a straight line with slope and intercept equal to $-\Delta H°/R$ and $\Delta S°/R$, respectively. Here the values of $\Delta H°$ and $\Delta S°$ were 12.09 kJ/mol and 100.15 J/mol K. The positive value of $\Delta H°$ confirm the endothermic nature of adsorption process, whereas the positive value of $\Delta S°$ suggests the high degree of freedom of adsorption system at equilibrium due to the interaction between active sites and metal ion.

$$\ln K_L = -\Delta H°/RT + \Delta S°/R \tag{7}$$

Gibbs free energy of adsorption ($\Delta G°$) was calculated from the following Eq. (8). The present values of $\Delta G°$ at 35, 45 and 55 °C were −18.76, −19.75 and −20.76 kJ/mol. The negative value of $\Delta G°$ indicates that the adsorption reaction is spontaneous. The observed increase in negative values of $\Delta G°$ with increasing temperature implies that the adsorption becomes more favorable at higher temperature. Actually, the values of $T\Delta S°$ is increasing with increasing temperature and $|\Delta H°| < |T\Delta S°|$. This indicates that the adsorption process is dominated by entropic rather than enthalpic changes [30].

$$\Delta G° = -\Delta H - T\Delta S° \tag{8}$$

On the optimum conditions for the uptake of Ni^{2+}, 10 trusses MFT/CFs were introduced in a flask, containing 50 mL spent electroless nickel plating bath with a binary mixture with 0. 1 M Pd^{2+}, Pb^{2+}, Ca^{2+} due to probably coexisting in the spent electroless

Table 3
Parameters of the pseudo-first order and pseudo-second order for the adsorption of Ni^{2+} on MFT/CFs.

Metal ion	$Q_{e,exp}$ (mM/g)	The pseudo-first order			Pseudo-second order		
		k_1 (min^{-1})	q_e (mM/g)	R^2	k_2 (g/mM min)	q_e (mM/g)	R^2
Ni^{2+}	0.81	0.0806	0.714	0.968	0.129	0.898	0.997

Table 4
Langmuir constants for adsorption of Ni^{2+}on MFT/CFs.

T (°C)	Q_{max} (mM/g)	K_L (L/mM)	R^2
35 °C	0.57	1.50	0.999
45 °C	0.69	1.76	0.999
55 °C	0.77	2.34	0.999

nickel plating baths. 5 mL of the solution was taken then filtrated off, where the residual concentration of Ni^{2+} was determined. The separation factor could be obtained using Eq. (9) [24]. Where C_{A1} (C_{B1}) and C_{A2} (C_{B1}) stand for the concentrations of A (B) before and after adsorption, respectively, here Ni^{2+} over the Pd^{2+}, Pb^{2+}, Ca^{2+} were to be 44.4, 2.3 and 120.6.

$$\text{Separation factor } (S_{A/B}) = (C_{A1} - C_{A2}) \times C_{B2}/(C_{B1} - C_{B2}) \times C_{A2} \quad (9)$$

Regeneration of MFT/CFS was investigated by repeated cycles of adsorption/desorption of Ni^{2+} in 5 mM EDTA/1 M HNO_3, during 24 h, under stirring, the desorption ratio was calculated from Eq. (10). The amounts of Ni^{2+} adsorption and recovery percentage from five consecutive adsorption/desorption cycles indicated desorption efficiency as high as 96%, and the Ni^{2+}-free MFT/CFs could be re-used after neutralization. At the 5th cycle, the adsorption capacity was found to be 39 ± 2 mg/g, which is 87% of that determined at the 1st cycle (45 ± 2 mg/g).

$$\text{Desorption ratio} = (\text{amount of desorbed } Ni^{2+}/\text{amount of adsorbed } Ni^{2+}) \times 100\% \quad (10)$$

4. Conclusions

Tetraoxalyl ethylenediamine modified melamine resin grafted-carbon fibers were obtained by compound electrochemical and organic synthesis methods. Electrochemistry, kinetic and thermodynamics studies illustrated that the functional CFs could selectively separate Ni^{2+} form the spent electroless nickel plating baths accompanying the formation of nano-nickel coated-carbon fibers material. Thermodynamic data indicated that the adsorption process is endothermic spontaneous reaction. Kinetic analysis showed that the adsorption of Ni^{2+} on MFT/CFs is perfectly fit pseudo-second order model. The interaction mechanism between metal ion and active sites has been interpreted as chelation. This work provided a very efficient and convenient approach for exploring promising chelate resin coated-carbon fibers materials on nickel recovery from the spent electroless nickel plating baths.

Acknowledgments

This work was supported by the National Natural Science Foundation of China (NSFC, 21076054); Natural Science Important Foundation of Educational Commission of Anhui Province (2010AJZR-85, 2011AJZR-87).

References

[1] A. Brenner, Reminiscences of early electroless plating, Plat. Surf. Finish. 71 (1984) 24–27.
[2] R.E. Miller, Trends in the electroless nickel industry, Plat. Surf. Finish. 74 (1987) 52–56.
[3] D.W. Grosse, A review of alternative treatment processes for metal bearing hazardous waste streams, J. Air. Pollut. Control Assoc. 36 (1986) 603–614.
[4] K. Parker, Waste treatment of spent electroless nickel baths, Plat. Surf. Finish. 70 (1983) 52–55.
[5] F. Levy, K. Doss, Regeneration of electroless nickel solution by ion exchange, Plat. Surf. Finish. 74 (1987) 80–81.
[6] T. Sana, K. Shiomori, Y. Kawano, Extraction rate of nickel with 5-dodecylsalicylaldoxime in a vibro-mixer, Sep. Purif. Technol. 44 (2005) 160–165.
[7] M. Tanaka, H. Narita, Y. Sato, Improvement of the extraction and stripping rates of nickel in the solvent extraction system with LIX84I, J. MMIJ 120 (2004) 440–445.
[8] Y. Kuboi, R.Takeshita, Extension of bath life by electrodialysis method at electroless nickel plating baths, in: American EN 89 Conference, New York, 1989, p. 59.
[9] S. Madhavakrishnan, K. Manickavasagam, K. Rasappan, P.S.S. Shabudeen, R. Venkatesh, S. Pattabhi, Ricinus communis pericarp activated carbon used as an adsorbent for the removal of Ni(II) from aqueous solution, E-J. Chem. 5 (2008) 761–769.
[10] K. Kadirvelu, K. Thamaraiselvi, C. Namasivayam, Adsorption of nickel(II) from aqueous solution onto activated carbon prepared from coirpith, Sep. Purif. Technol. 24 (2001) 497–505.
[11] R. Idhayachander, K. Palanivelu, Electrolytic recovery of nickel from spent electroless nickel bath solution, E-J. Chem. 7 (2010) 1412–1420.
[12] G. Orhan, C. Arslan, H. Bombach, M. Stelter, Nickel recovery from the rinse waters of plating baths, Hydrometallurgy 65 (2002) 1–8.
[13] <http://www.3158.cn/news/20090227/14/460736064-1.shtml>.
[14] S.M. Chergui, N. Abbas, T. Matrab, M. Turmine, E.B. Nguyen, R. Losno, J. Pinson, M.M. Chehimi, Uptake of copper ions by carbon fiber/polymer hybrids prepared by tandem diazonium salt chemistry and in situ atom transfer radical polymerization, Carbon 48 (2010) 2106–2122.
[15] K.K. Kara, D. Sathiyamoorthyb, The nickel–phosphorous (Ni–P) coating on carbon fiber was studied, using sodiumhypophosphite as a reducing agent in alkaline medium, J. Mater. Process. Technol. 209 (2009) 3022–3029.
[16] S. Arai, M. Endo, S. Hashizume, Y. Shimojima, Nickel-coated carbon nano fibers prepared by electroless deposition, Electrochem. Commun. 6 (2004) 1029–1031.
[17] H. Xu, L. Zeng, D. Huang, Y. Xian, L. Jin, A Nafion-coated bismuth film electrode for the determination of heavy metals in vegetable using differential pulse anodic stripping voltammetry: an alternative to mercury-based electrodes, Food Chem. 109 (2008) 834–839.
[18] M.A.A.A. El-Ghaffar, Z.H. Abdel-Wahab, K.Z. Elwakeel, Extraction and separation studies of silver(I) and copper(II) from their aqueous solution using chemically modified melamine resins, Hydrometallurgy 96 (2009) 27–34.
[19] A.M. Naser, A.A. Salman, I.M. Abd-Ellah, M.A. Abd El-Ghaffar, A.N. Khouzondar, New metal complex pigments, J. Oil Colour Chem. Assoc. 63 (1980) 337–339.
[20] G.P. Jin, Y.F. Ding, P.P. Zheng, Electrodeposition of nickel nanoparticles on functional MWCNT surfaces for ethanol oxidation, J. Power Sources 166 (2007) 80–86.
[21] A.I. Balabanovich, The effect of melamine on the combustion and thermal decomposition behaviour of poly(butylene terephthalate), Polym. Degrad. Stab. 84 (2004) 451–458.
[22] A. Deepatana, M. Valix, Comparative adsorption isotherms and modeling of nickel and cobalt citrate complexes onto chelating resins, Desalination 218 (2008) 334–342.
[23] T.S. West, Complexometry with EDTA and Related Reagents, BDH, third ed., Chemicals Ltd., 1969.
[24] Y.S. Ho, G. McKay, Pseudo-second order model for sorption processes, Process Biochem. 34 (1999) 451–465.
[25] E. Guibal, C.J. Milot, M. Tobin, Metal-Anion sorption by chitosan beads: equilibrium and kinetic studies, Ind. Eng. Chem. Res. 37 (1999) 1454–1463.
[26] S. Lagergren, Zur theorie der sogenannten adsorption gelöster stoffe. Kungliga Svenska Vetenskapsakademiens, Handlingar 24 (1898) 1–39.
[27] J. Gong, T. Liu, X. Wang, X. Hu, L. Zhang, Efficient removal of heavy metal ions from aqueous systems with the assembly of anisotropic layered double hydroxide nanocrystals at carbon nanosphere, Environ. Sci. Technol. 45 (2011) 6181–6187.
[28] L. Qi, Z. Xu, Lead sorption from aqueous solutions on chitosan nanoparticles, J. Colloid Interface Sci. 251 (2004) 186–193.
[29] J. Tellinghuisen, Van't Hoff analysis of K° (T): How good...or bad?, Biophys Chem. 120 (2006) 114–120.
[30] A.M. Donia, A.A. Atia, K.Z. Elwakeel, Recovery of gold(III) and silver(I) on a chemically modified chitosan with magnetic properties, Hydrometallurgy 87 (2007) 197–206.